Optimal Dynamic Design of Anthropomorphic Robot Module with Redundant Actuators

Sang Heon Lee*, Byung-Ju Yi and Yoon Keun Kwak*****

(Received July 14, 1995)

In this paper, a study on the optimal dynamic design for an anthropomorphic robot module with redundant actuators is performed. Musculoskeletal structure of human body is a typical example of redundantly actuated mechanism, and provides superior features than general robotic mechanisms. An anthropomorphic robot module that resembles the structure of human upper limb is introduced to utilize the advantages of redundant actuation system. Optimal dynamic design of the proposed robot module that follows optimal kinematic design is carried out to maximize the advantages. Five design indices are introduced, which are associated with inertia matrix, inertia power array representing nonlinear terms and gravity terms of the dynamic modeling equation. A concept of composite design index based on max-min principle of fuzzy theory is employed to deal with multi-criteria based design. As a result of dynamic optimization, a set of dynamic parameters, representing optimal mass distribution of the manipulator is obtaind. It is shown that the dynamic optimization yields a notable enhancement in dynamic performances, as compared to the case of kinematic optimization only.

Key Words: Redundant Actuation System, Dynamic Optimization, Dynamic Composite Design Index, Anthropomorphic Robot Module, Multi-criteria Based Design

1. Introduction

In the design of robot manipulators, kinematic optimization has been regarded as an important procedure to enhance operational performances of robot manipulator. Recently, dynamic performances have been considered as other significant design factors, and therefore optimal dynamic design is emphasized to achieve improvement of dynamic performances. Youcef-Toumi and Asada (1987) suggested a design that the inertial matrix becomes diagonal and/or invariant for an arbitrary arm configuration. Park and Cho (1991) proposed a redesign method and applied to PUMA 560 robot, and achieved a less configuration-variant and less nonlinear dynamic characteristics by simplifying the dynamic model. Singh and Rastegar (1992) suggested a concept, referred to as the global inertia ellipsoid that represents the global inertial characteristics of a manipulator. They showed examples of optimal synthesis of manipulators based on the global inertia ellipsoid.

In this study, optimal dynamic design of an anthropomorphic robot module with redundant actuators is performed. Studies on redundant actuation system have been received much attention since redundant actuation mode can provide several beneficial operations such as load sharing and internal load generation. In the previous work, it was shown that the redundantly actuated manipulator is superior to the nonredundant ones in terms of several operational performances (Lee,

* Graduate Student, Department of Mechanical Engineering, Korea Advanced Institute of Science and Technology, 373-1 Kusong-dong, Yusong-gu, Taejon, 305-701 Korea

** Department of Control and Instrumentation Engineering, Hanyang University, 396 Taehak-dong, Ansan, Kyungki, 425-791 Korea

*** Department of Mechanical Engineering, Korea Advanced Institute of Science and Technology, 373-1 Kusong-dong, Yusong-gu, Taejon, 305-701 Korea

et. al., 1995). Figure 1 shows an anthropomorphic robot module resembling musculoskeletal structure of the human upper limb. The robot module is redundantly actuated by translational actuators as the human upper limb. The kinematic optimization has been carried out with the same robot module in the previous work by the present authors (Lee, et. al., 1994).

A dynamic optimization is additionally performed for this module to maximize the enhancement of operational performances obtained by redundant actuation, following kinematic optimization. Five dynamic design indices associated with the dynamic model of the robot manipulator are introduced. The indices are operational acceleration, operational velocity and their gradients. They represent operational velocity and acceleration capacity, gravity load magnitude on actuators and uniformity of distribution for the local design index over the workspace. To cope with the multi-criteria based optimal design, a concept of dynamic composite design index is employed. The dynamic composite design index is constructed by integrating the design indices into one value, based on max-min principle of fuzzy theory. A set of inertial parameters that represents optimal mass distribution of the links is obtained from the dynamic optimization result. The dynamically optimized manipulator is compared with the kinematically optimized but dynamically nonoptimized one with respect to dynamic design indices and three operational performances such as maximum load handling capacity, maximum hand velocity and maximum hand acceleration. The comparison results show that the dynamic optimization gives a notable enhancement of operational performances. Consequently, it is concluded that dynamic optimization is an another significant step to enhance the operational performance, following kinematic optimization.

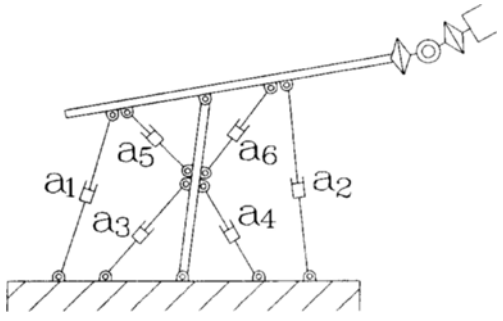

Fig. 1 Two degree-of-freedom anthropomorphic robot module

2. Musculoskeletal Structure of the Human Upper Limb

A human arm consists of 29 muscles (Spence, 1986), showing redundancy in actuation compared to seven joint space freedoms and six operational space freedoms. It is presumed that the human arm utilizes these abundant force redundancies to optimize several objectives. A planar two-segment abstraction of the upper limb (e.g., the forearm and arm) is illustrated in Fig. 2. In this conceptual model, the skeletal segments are considered to be rigid bodies and the muscles are each assumed to have a single point of origin and insertion. Two types of biomechanical actuators are shown. The one is bi-articular muscle crossing two joints, and the other is mono-articular muscle crossing only one joint.

In Fig. 1, each link corresponds to human skeleton and the translational actuators corre-

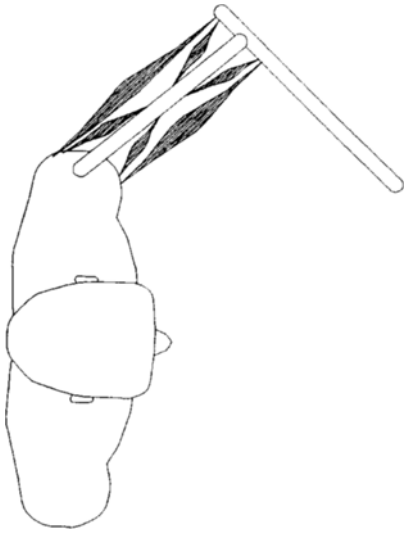

Fig. 2 Two-segment model of the human upper limb

spond to bi-articular and mono-articular muscles. Hogan (1985) investigated the spring-like behavior for this module. Yi and Freeman (1991) developed a mathematical model of the spring-like property for this module. In this study, optimal distribution of inertial parameters of this robot module is investigated in order to enhance the overall operational performances.

3. Kinematic/Dynamic Modeling

A kinematic constraint-embedding procedure (Kang et. al., 1990) is employed for explicit dynamic modeling of general closed-loop type robot systems, in terms of a minimum coordinate set. Initially, the closed-loop type manipulator is assumed to have an open-tree structure, and the open-chain dynamics can be directly incorporated into the closed-chain dynamics by using the principle of virtual work.

3.1 Kinematic modeling

The whole joint set of the system represented in Lagrangian coordinate is given as $\boldsymbol{\phi}_P$, and the set of actuated joints is defined as $\boldsymbol{\phi}_A$ which is the subset of $\boldsymbol{\phi}_P$. For redundantly actuated closed-loop mechanisms, $\boldsymbol{\phi}_A$ will be represented as below.

$$\boldsymbol{\phi}_A=[\boldsymbol{\phi}_s^T,\ \boldsymbol{\phi}_a^T]^T \tag{1}$$

where $\boldsymbol{\phi}_a$ denotes the set of minimum coordinates and its dimension is the same as the kinematic degree-of-freedom of the system, and $\boldsymbol{\phi}_s$ denotes the set of redundantly actuated joints.

The velocity vector for the whole Lagrangian joints is related to the set of minimum coordinates as

$$\dot{\boldsymbol{\phi}}_p=[\ \boldsymbol{G}_a^p]\ \dot{\boldsymbol{\phi}}_a \tag{2}$$

where $[\boldsymbol{G}_a^p]$ is the first-order Kinematic Influence Coefficient (KIC) representing the relationship between $\dot{\boldsymbol{\phi}}_p$ and $\dot{\boldsymbol{\phi}}_a$. The velocity vector at the end-effector ($\dot{\boldsymbol{u}}$) is obtained by substituting the information of Eq. (2) into an open-chain kinematic relation, as

$$\dot{\boldsymbol{u}}=[\boldsymbol{G}_a^u]\dot{\boldsymbol{\phi}}_a \tag{3}$$

where $[\boldsymbol{G}_a^u]$ is the first-order KIC representing the relationship between $\dot{\boldsymbol{u}}$ and $\dot{\boldsymbol{\phi}}_a$. Reversely, $\dot{\boldsymbol{\phi}}_a$ can be represented as a function of $\dot{\boldsymbol{u}}$.

$$\dot{\boldsymbol{\phi}}_a=[\boldsymbol{G}_u^a]\dot{\boldsymbol{u}}=[\boldsymbol{G}_a^u]^{-1}\dot{\boldsymbol{u}} \tag{4}$$

A force equilibrium equation between the force vector at the end-effector ($\boldsymbol{T}_u$) and the force vector at the minimum coordinates ($\boldsymbol{T}_a$) is given as

$$\boldsymbol{T}_u=[\boldsymbol{G}_u^a]^T\ \boldsymbol{T}_a \tag{5}$$

An acceleration vector at the set of minimum coordinates is obtained by differentiating Eq. (4) with respect to time, as

$$\ddot{\boldsymbol{\phi}}_a=[\boldsymbol{G}_u^a]\ \ddot{\boldsymbol{u}}+\dot{\boldsymbol{u}}^T[\boldsymbol{H}_{uu}^a]\dot{\boldsymbol{u}} \tag{6}$$

where $[\boldsymbol{H}_{uu}^a]$ is the second-order KIC representing the relationship between $\ddot{\boldsymbol{\phi}}_a$ and $\dot{\boldsymbol{u}}$, defined as

$$[\boldsymbol{H}_{uu}^a]=\frac{\partial}{\partial \boldsymbol{u}}([\boldsymbol{G}_u^a]) \tag{7}$$

A force equilibrium equation between the force vector at the end-effector ($\boldsymbol{T}_u$) and the force vector at the actuated joints ($\boldsymbol{T}_A$), can be represented as

$$\boldsymbol{T}_u=[\boldsymbol{G}_u^A]^T\boldsymbol{T}_A \tag{8}$$

where the first-order KIC representing the relationship between $\dot{\boldsymbol{\phi}}_A$ and $\dot{\boldsymbol{u}}$ is defined as

$$[\boldsymbol{G}_u^A]=[\boldsymbol{G}_a^A][\boldsymbol{G}_u^a] \tag{9}$$

where $[\boldsymbol{G}_a^A]$ is a subset of $[\boldsymbol{G}_a^p]$, defined in Eq. (2), and $[\boldsymbol{G}_u^a]$ is defined in Eq. (4). $[\boldsymbol{G}_u^A]^T$ is not symmetric, since the dimension of $\boldsymbol{T}_A$ is greater than $\boldsymbol{T}_u$, so $\boldsymbol{T}_A$ has infinite solutions. $\boldsymbol{T}_A$ of Eq. (10) is obtained in such a way that the 2-norm $\|\boldsymbol{T}_A\|_2$ is minimized

$$\boldsymbol{T}_A=[\boldsymbol{G}_A^u]^T\boldsymbol{T}_u=([\boldsymbol{G}_u^A]^T)^+\boldsymbol{T}_u \tag{10}$$

where $[\boldsymbol{G}_A^u]^T$ is defined as (Strang, 1980)

$$\begin{aligned}[\boldsymbol{G}_A^u]^T&=([\boldsymbol{G}_u^A]^T)^+\\&=[\boldsymbol{G}_u^A]([\boldsymbol{G}_u^A]^T[\boldsymbol{G}_u^A])^{-1}\end{aligned} \tag{11}$$

In this work, we employ the solution of Eq. (11) in the resolution of force redundancies.

3.2 Dynamic modeling

A dynamic model at the set of minimum coordinates is given as

$$\boldsymbol{T}_a=[\boldsymbol{I}_{aa}^*]\ddot{\boldsymbol{\phi}}_a+\dot{\boldsymbol{\phi}}_a^T\ [\boldsymbol{P}_{aaa}^*]\dot{\boldsymbol{\phi}}_a \tag{12}$$

where $[\boldsymbol{I}_{aa}^*]$ denotes the inertia matrix, and $[\boldsymbol{P}_{aaa}^*]$ denotes the inertia power array representing the effects of Coriolis force and centrifugal force.

In the dynamic optimization procedure, we employ a dynamic equation which relates T_a to $\ddot{u}$ and $\dot{u}$. The dynamic equation can be obtained by substituting Eqs. (4) and (6) into Eq. (12), as

$$T_a=[I^*_{au}]\ddot{u}+\dot{u}^T[P^*_{auu}]\dot{u} \tag{13}$$

where

$$[I^*_{au}]=[I^*_{aa}][G^a_u] \tag{14}$$

$$[P^*_{auu}]=[I^*_{aa}]\circ[H^a_{uu}]+[G^a_u]^T[P^*_{aaa}][G^a_u] \tag{15}$$

$[I^*_{au}]$ represents the effect of $\ddot{u}$ upon T_a, while $[P^*_{auu}]$ represents the effect of $\dot{u}$ upon the T_a. '$\circ$' of Eq. (15) denotes a generalized scalar dot product (Freeman and Tesar, 1988).

Also, the dynamic model representing the relationship between the force vector at the actuated joints (T_A) and the end-effector motion ($\ddot{u}$ and $\dot{u}$) is obtained by substituting Eq. (13) into Eq. (10), as

$$T_A=[G^u_A]^T T_u=[G^u_A]^T[G^a_u]^T T_a =[I^*_{Au}]\ddot{u}+\dot{u}^T[P^*_{Auu}]\dot{u} \tag{16}$$

where

$$[I^*_{Au}]=[G^u_A]^T[G^a_u]^T[I^*_{au}]=[G^a_A]^T[I^*_{au}] \tag{17}$$

$$[P^*_{Auu}]=([G^u_A]^T[G^a_u]^T)\circ[P^*_{auu}] =[G^a_A]^T\circ[P^*_{auu}] \tag{18}$$

4. Dynamic Design Index

Five design indices considered for the optimal dynamic design are operational acceleration index, operational velocity index, gravity load index and gradient design indices for operational acceleration index and operational velocity index. The indices obtained from the dynamic models of Eqs. (14) and (15) represent operational velocity and acceleration capacity, gravity load magnitude on actuators and uniformity of the index's distribution over the workspace, respectively.

Operational acceleration index is considered first. It is defined as the maximum eigenvalue of $[I^*_{au}]$, and quoted as λ_I. $[I^*_{au}]$ is function of manipulator configuration, and λ_I is local value that varies as the configuration changes. So the global operational acceleration index is defined to represent the overall acceleration capacity throughout the workspace. The global design indices are used in optimization procedure to reflect global dynamic characteristics into the design. The global operational acceleration index is defined as the average of the λ_I's over the entire workspace, and is defined as

$$\Lambda_I=\frac{\int_W \lambda_I \mathrm{d}W}{\int_W \mathrm{d}W} \tag{19}$$

where W denotes the workspace area. Note that the larger λ_I, the larger actuating force is needed for a given unit operational acceleration. Therefore, Λ_I should be minimized.

Second design index is operational velocity index that is related to the velocity capacity of the manipulator. This index is obtained from $[P^*_{auu}]$ that has two planes for a two degree-of-freedom system. The operational velocity index is defined as the average of the maximum eigenvalues for the two planes of $[P^*_{auu}]$.

$$\lambda_P=\frac{1}{2}\sum_{i=1}^{2}(\lambda_i)_{\max} \tag{20}$$

where $(\lambda_i)_{\max}$ is the maximum eigenvalue of ith plane of $[P^*_{auu}]$. λ_P is also local value, so the global index is needed to be defined. The global operational velocity index is defined as the average of λ_P's over the workspace.

$$\Lambda_P=\frac{\int_W \lambda_P \mathrm{d}W}{\int_W \mathrm{d}W} \tag{21}$$

The larger λ_P, the larger actuating force is needed for a given unit operational velocity. Consequently, Λ_P should be minimized.

The third design index represents the magnitude of gravity load exerted on the actuators, and the gravity load index is defined as the 2-norm of gravity load vector, quoted as τ_G. The global gravity load index is defined as the maximum value of τ_G's throughout the workspace, and is given as the form of following infinity norm

$$T_G=\{\sum^{W}(\tau_G)^{\infty}\}^{1/\infty} \tag{22}$$

Note that the larger τ_G, the larger actuating force is needed to withstand the gravity load on the actuators. Therefore, T_G should be minimized.

Other two design indices are gradient prop-

erties for λ_I and λ_P. The values of λ_I and λ_P vary as the manipulator configuration changes, and gradient design index represents the change rate of the local design index. Gradient design index should be considered in order for the given dynamic design indices to be evenly distributed throughout the workspace. The procedure to evaluate the gradient design index is given as follows. First, the workspace is divided into rectangular meshes with 0.1 m interval in this work, and local gradient design index is defined as the difference between the design indices obtained at adjacent two points. The maximum value of the local gradient design indices throughout the workspace is defined as the global gradient design index. The global gradient design index for λ_I is defined as

$$\Lambda_I^G=(\sum^W | \lambda_I^G |^\infty)^{1/\infty} \tag{23}$$

where λ_I^G denotes the local gradient design index for λ_I. In a similar fashion, the local gradient design index for λ_P is denoted as λ_P^G, and its global gradient design index is defined as

$$\Lambda_P^G=(\sum^W | \lambda_P^G |^\infty)^{1/\infty} \tag{24}$$

The smaller the global gradient design indices, the better uniformly distributed the dynamic performances throughout the workspace. So, the global gradient design indices should be minimized.

In order to cope with multi-criteria based design, we employ a concept of dynamic composite design index. Various design indices introduced above are usually incommensurate concepts due to differences in unit and physical meanings, and therefore should not be combined with normalization and weighting functions unless they are transferred into a common domain. As an initial step to this process, preferential information should be given to each design parameter and each design index. Then, each design index is transferred to a common preference design domain which ranges from zero to one. Here, the preference given to each design criterion is very subjective to the designer. Preference can be given to each criterion by weighting. This provides flexibility in design. For Λ_I, the best preference is given the minimum value, and the least preference is given the maximum value of the criterion, the design index is transferred into common preference design domain as below.

$$\tilde{\Lambda_I}=\frac{(\Lambda_I)_{\max}-\Lambda_I}{(\Lambda_I)_{\max}-(\Lambda_I)_{\min}} \tag{25}$$

where '~' implies that the index is transferred into the common preference design domain. Since the rest of indices mentioned are also in favor of minimum value, $\tilde{\Lambda_P}$, $\tilde{\mathbf{T}_G}$, $\tilde{\Lambda_I^G}$, and $\tilde{\Lambda_P^G}$ are obtained by the same fashion of Eq. (25). The decision of the preference level on the maximum and minimum values of each design index is subject to the designer's choice.

A set of optimal design parameters is obtained based on max-min principle of fuzzy theory (Klir and Folger, 1988). Initially, the minimum values among the design indices for all set of design parameters are obtained, and then a set of design parameters, which has the maximum of the minimum values, is chosen as the optimal set of design parameters. Based on this principle, the dynamic composite design index (*DCDI*) is defined as the minimum value of the above mentioned design indices at a set of design parameters, and is given as

$$DCDI=[(\Lambda_I)^\alpha,\ (\tilde{\Lambda_P})^\beta,\ (\tilde{\mathbf{T}_G})^\gamma,\ (\tilde{\Lambda_I^G})^\delta,\ (\tilde{\Lambda_P^G})^\varepsilon] \tag{26}$$

The upper Greek letters (α, β, *etc.*) represent the degrees of weighting, and usually large value implies large weighting. In general, the value of weighting is determined based on fuzzy measure such as normal, very, more or less, absolutely, and so on. Though those fuzzy measures can be defuzzified as crisp values very subjectively, the following cases have been employed; normal is equivalent to 1, very is equivalent to 2, more or less is equivalent to 0.5, absolutely is equivalent to ∞, and so on (Klir and Folger, 1988). In order to evenly satisfy the several design objectives for all design indices, all of the weighting factors are set to 1.0. Now, a set of optimal design parameters is chosen as the set that has the maximum *DCDI* among all *DCDI*'s calculated for all set of design parameters.

5. Optimal Dynamic Design

Mass of link, position of mass center, mass moment of inertia, *etc.* can be cited as dynamic design parameters of manipulator. Figure 3 shows three dynamic parameters of the robot module. In this paper, the dynamic design parameters are m_1, r_1 and r_2. We assume that the links of the manipulator have the shape of hollow cone and have uniform mass density. Variations of r_1 and r_2 result in the change of mass moment of inertia and the position of mass center (L_c) of each link. Three constraints for r_1 and r_2 are given as

$$r_1 + R_1 = 0.10 \ m \tag{27}$$

$$r_2 + R_2 = 0.10 \ m \tag{28}$$

$$0.03 \ m \leq r_1, r_2 \leq 0.07 \ m \tag{29}$$

R_i and L_{ci} decrease as r_i increases, and this transition results in the reduction of the gravity and inertial loads exerted on the actuators. The mass moment of inertia with respect to mass center is maximum when r_i is equal to R_i, and decreases as the difference between r_i and R_i increases. Dynamic characteristics of the manipulator will also vary by changing the ratio between m_1 and m_2, under the following constraint equations

$$m_1 + m_2 = m_{total} = 15.0 \ kg \tag{30}$$

$$4.0 \ kg \leq m_1 \leq 11.0 \ kg \tag{31}$$

A small m_1 results in a large m_2, and consequently large actuator capacity is needed to withstand the increased inertial load. The data for Eqs. (27)~(31) are chosen from KIRO-4 robot (Lee, et. al., 1993) which was developed in the Department of Mechanical Engineering at KAIST (Korea Advanced Institute of Science and Technology).

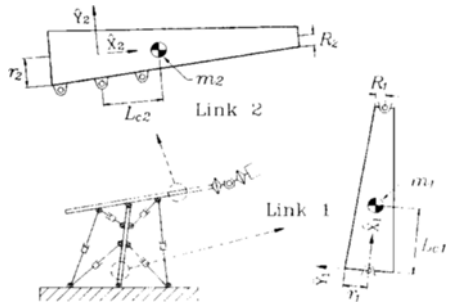

Fig. 3 Dynamic parameters of the robot module

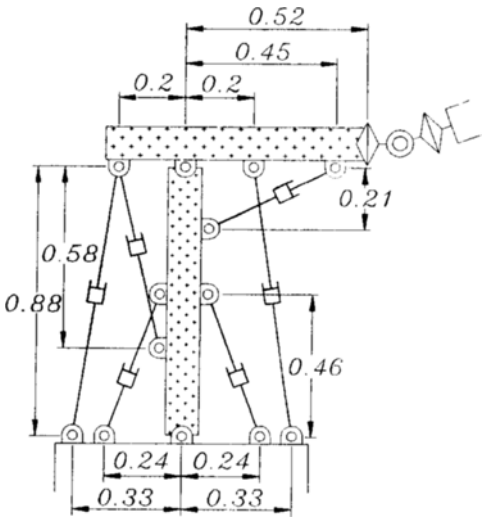

Fig. 4 Kinematic parameters of the kinematically optimized manipulator (Unit : meter)

The kinematic optimization for this manipulator was performed by present authors (Lee, et. al., 1994). The kinematic parameters obtained from the kinematic optimization procedure are used in the dynamic optimization. Kinematic dimensions of the manipulator is shown in Fig. 4. Note that

Table 1 Inertial parameters of the maniulator

Design Cases	Dynamic Design Parameters		
	m_1	r_1	r_2
Dynamically Nonoptimized Case	8.00 kg	0.050 m	0.050 m
Dynamically Optimized Case	11.00 kg	0.070 m	0.031 m

the shape of the two links is cylindrical in optimal kinematic design.

To deal with a nonlinear optimization with constraints, three numerical methods are used. The exterior penalty function method is employed to transform the constrained optimization problem into an unconstrained optimal problem. Next, Powell's method is applied to obtain an optimal solution for the unconstrained problem, and quadratic interpolation method is utilized for uni-directional minimization (Yuan-Chou, 1985).

The optimization results for this design are shown in Table 1. The shape of the dynamically optimized manipulator is shown in Fig. 5.

The result of the dynamic optimization is evaluated by two ways. Initially, the trends of dynamic design indices are observed in order to show how much the dynamic performances can be improved. It is seen from Fig. 6 and Fig. 7 the magnitudes of the first three dynamic indices resulting from the dynamic optimization have been decreased throughout workspace, as compared to those of dynamically nonoptimized case. In these contour plot, X coordinates indicates horizontal position in the workspace and Y coordinates cooresponds to vertical position. The curved lines connects the points have the same value of the index, so the index value changes rapidly as the configuration varies in where an interval between lines is narrow. Reversely, where

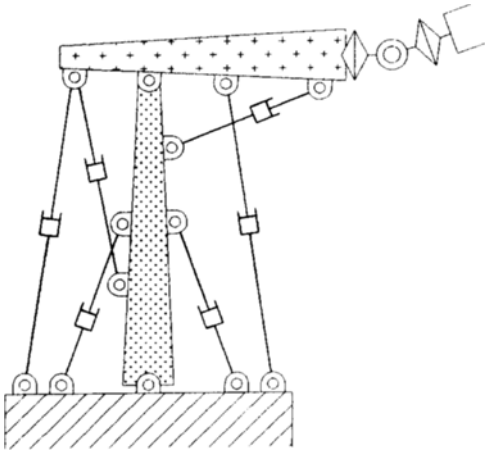

Fig. 5 Schematic diagram of the dynamically optimized manipulator

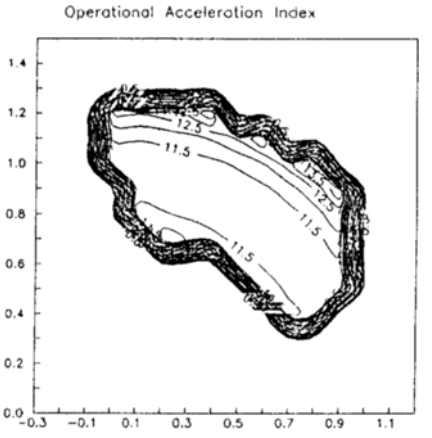

(a) Operational acceleration index

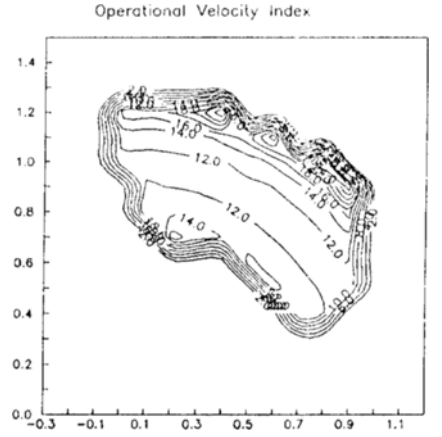

(b) Operational velocity index

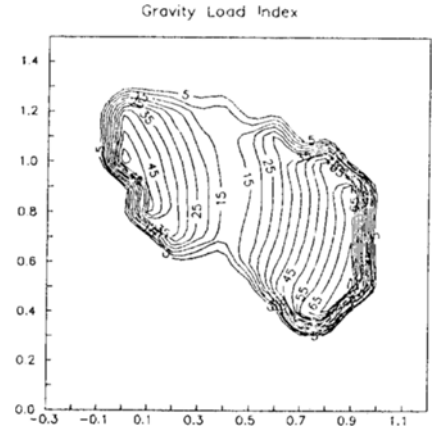

(c) Gravity load index

Fig. 6 Distribution of the dynamic design index over the workspace for kinematically optimized manipulator

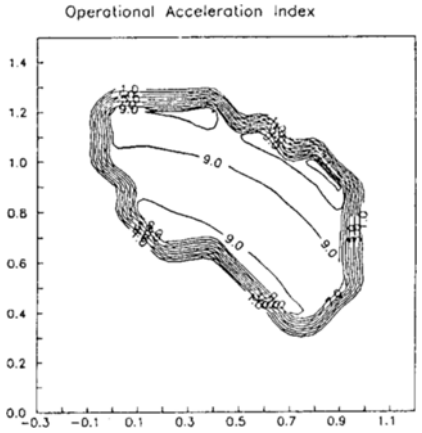

(a) Operational acceleration index

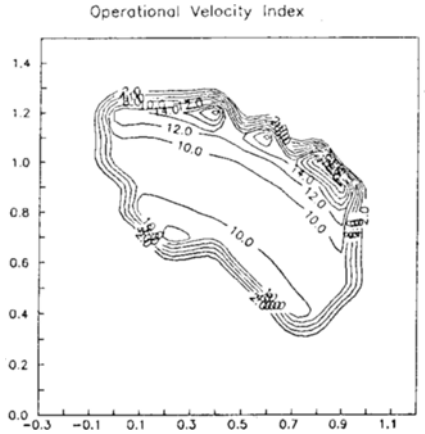

(b) Operational velocity index

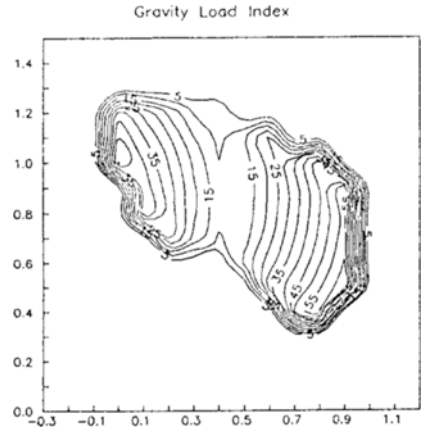

(c) Gravity load index

Fig. 7 Distribution of dynamic design index over the workspace for dynamically optimized manipulator

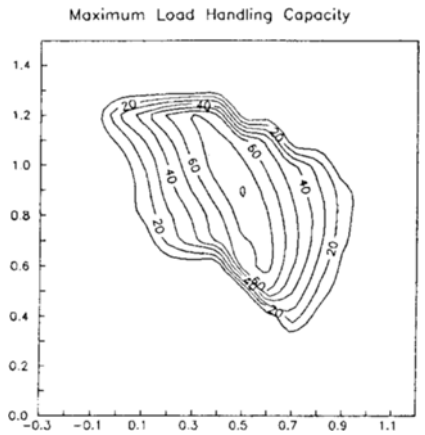

(a) Maximum load handling capacity

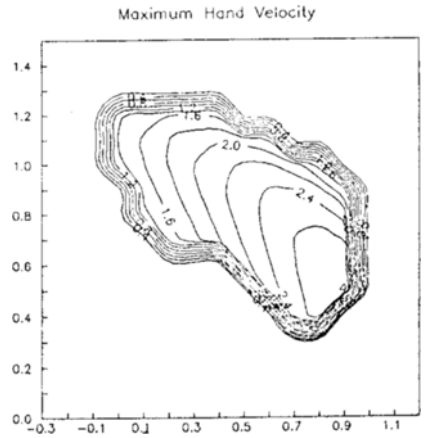

(b) Maximum hand velocity

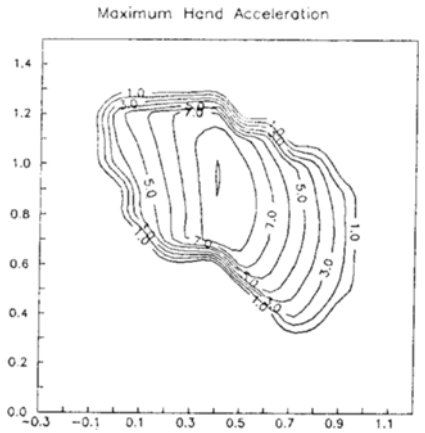

(c) Maximum hand acceleration

Fig. 8 Operational performance distribution of the kinematically optimized manipulator

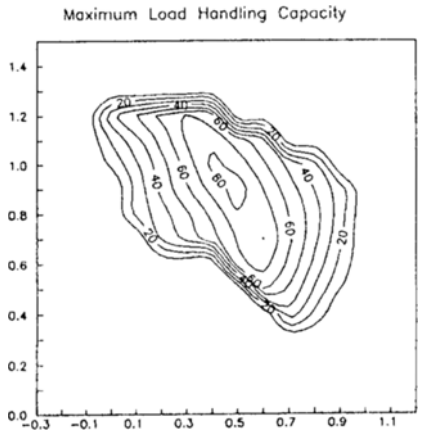

(a) Maximum load handling capacity

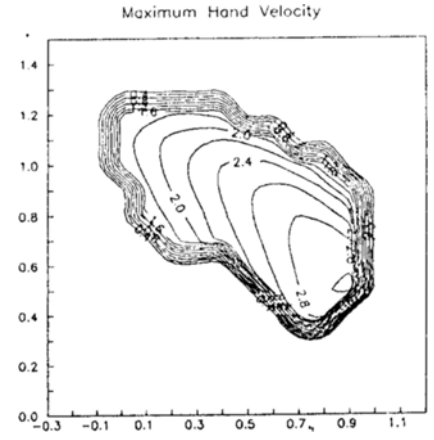

(b) Maximum hand velocity

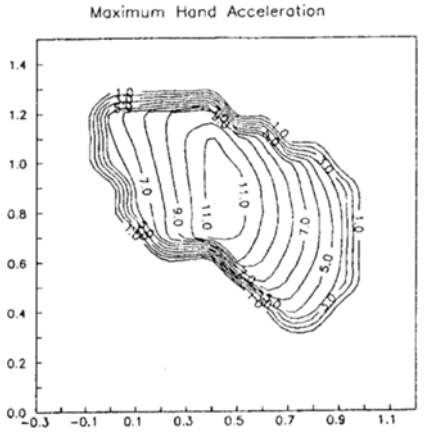

(c) Maximum hand acceleration

Fig. 9 Operational performance distribution of the dynamically optimized manipulator

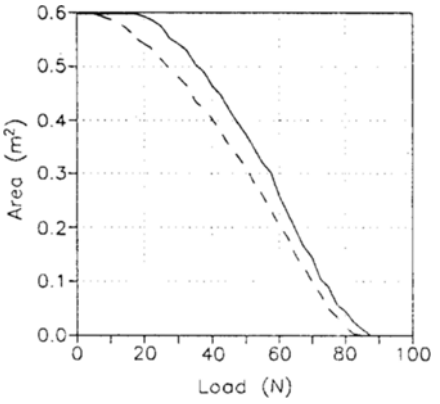

(a) Maximum load handling capacity

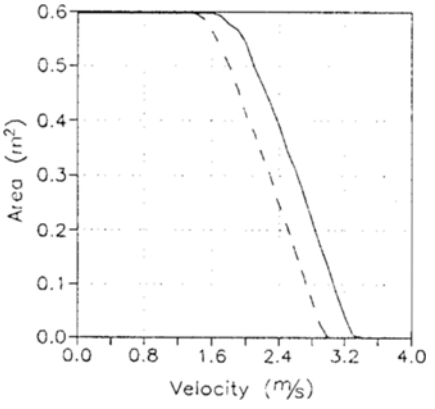

(b) Maximum hand velocity

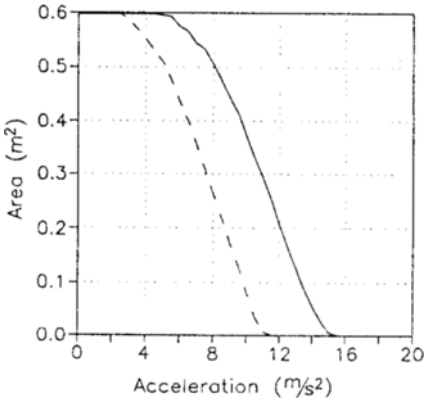

(c) Maximum hand acceleration

Fig. 10 Enable wokspace area for the operational performance (- - - : dynamically nonoptimized case; ----- : dynamically optimized case)

an interval is wide, the index is changeless. The shape of distribution for each dynamic index does not change, but the amount of reduction is about from 10% through 20%. This denotes the enhancement of the dynamic characteristics of the manipulator.

Secondly, three operational performances are adopted to evaluate the dynamic performances of this manipulator. They include maximum load handling capacity, maximum hand velocity, and maximum hand acceleration (refer to Appendix for the detailed descriptions). Given the sizes of all system actuators as 100.0 N, dynamic performances of dynamically optimized case are compared to those of dynamically nonoptimized case. It is observed from Fig. 8 and Fig. 9 that the magnitude of all three-operational performances have been increased throughout the workspace. This denotes the enhancement of dynamic performances resulting from the inclusion of dynamic optimization. In order to clearly distinguish the differences between the two cases, each dynamic performance is analyzed through an area-based plot. It is shown from Fig. 10 that the dynamically optimized case has more areas with higher payload than the kinematically optimized case has. The same trends can be observed for the operational hand velocity and operational hand acceleration.

6. Conclusion

In this study, a robot module that resembles the musculoskeletal structure of human upper limb is proposed to utilize the advantages of redundant actuation system. To maximize the advantages, the optimal dynamic design for the two degree-of-freedom anthropomorphic robot module with redundant actuators is performed. Five dynamic design indices representing the dynamic characteristics of the manipulator are introduced. The design indices are operational acceleration index, operational velocity index, gravity design index and gradient design indices for operational acceleration index and operational velocity index, and they are defined from the dynamic modeling equation of the robot module. To deal with a multi-criteria based design, a concept of composite design index based on max-min principle of fuzzy theory is employed.

As the result of dynamic optimization, we obtain a set of dynamic parameters, representing optimal mass distribution of the manipulator. In order to show the enhancement of the dynamic performances, the trends of the dynamic design indices and three operational dynamic performances are observed for both the dynamically optimized case and dynamically nonoptimized case. It is shown that the dynamic optimization provides a notable enhancement in dynamic performances, as compared to the case of kinematic optimization only. We concludes that the dynamic optimization of manipulator should be recognized as another significant procedure to enhance the overall operational performances of manipulators. The algorithm introduced in this work can also be applied to the design of general robotic manipulators.

References

Freeman, R. A. and Tesar, D., 1988, "Dynamic Modeling of Serial and Parallel Mechanisms/ Robotic Systems, Part I-Methodology, Part II-Applications," *Proc. 20th ASME Biennial Mechanisms Conf.*, DE-Vol. 15-3, pp. 7~27.

Hogan, N., 1985, "The Mechanics of Multi-Joint Posture and Movement Control," *Biological Cybernetics*, Vol. 52, pp. 315~331.

Kang, H. J., Yi, B-J., Cho, W. and Freeman, R. A., 1990, "Constraint-Embedding Approaches for General Closed-Chain System Dynamic in Terms of a Minimum Coordinate Set," *The 1990 ASME Biennial Mechnism Conf.*, DE-Vol. 24, pp. 125~132.

Klir, G. J. and Folger, T. A., 1988, *Fuzzy Sets, Uncertainty, and Information*, Prentice Hall, U. S.A., p. 31.

Lee, D. G., Jeong, K. S., Kim, K. S. and Kwak, Y. K., 1993, "Development of the Anthropomorphic Robot with Carbon Epoxy Composite Materials," *Composite Structures*, Vol. 8, No. 5, pp. 644~651.

Lee, S. H., Yi, B-J. and Kwak, Y. K., 1994,

"Optimal Design of Closed-Loop Type Robot Module with Redundant Actuation," *2nd IFAC/IFIP/IFORS Workshop on Intelligent Manufacturing System*, Vienna, pp. 569~573.

Lee, S. H., Yi, B-J. and Kwak, Y. K., 1995, "Performance Analysis and Optimal Actuator Sizing for Anthropomorphic Robot Module with Redundant Actuation," *Trans. of The Korean Society of Mechanical Engineers*, Vol. 19, No. 1, pp. 181~192.

Park, H. S. and Cho, H. S., 1991, "General Design Conditions for an Ideal Robotic Manipulator Having Simple Dynamics," *Int. J. Robotics Research*, Vol. 10, No. 1, pp. 21~29.

Singh, J. R. and Rastegar, J., 1992, "Optimal Synthesis of Robot Manipulators Based on Global Dynamic Parameters," *Int. J. of Robotics Research*, Vol. 11, No. 6, pp. 538~548.

Spence, P. A., 1986, *Basic human anatomy*, The Benjamin/Cummings Publishing Co. Inc., 2nd Ed.

Yi, B-J. and Freeman, R. A., 1991, "Modeling and Control of Impedance Properties in Biomechanical Systems," *Proc. ASME WAM, Advances in bioengineering*, BED-Vol. 20, pp. 521~524.

Youcef-Toumi, K. and Asada, H., 1987, "The Design of Open-Loop Manipulator Arms with Decoupled and Configuration-Invariant Inertia Tensors," *ASME J. Dynamic systems, Measurement, and Control*, Vol. 109, pp. 268~275.

Yuan-Chou, B. C., 1985, "Computer-Aided Optimization in the Dynamic Analysis and Parameteric Design of Robotic Manipulators," Ph.D. Thesis, Univ. of Florida, Gainsville.

Appendix

Maximum Load Handling Capacity is defined as *the maximum load that can be applied to the end-effector in any direction without exceeding actuation limit of any actuator* (Lee, *et. al.*, 1995).

The limits on the driving force T_{An} at the nth actuated joint are given as

$$(T_{An})_{\min} = -T_{An}^{M} + T_{An}^{G} \tag{A1}$$

$$(T_{An})_{\max} = T_{An}^{M} + T_{An}^{G} \tag{A1}$$

where T_{An}^{M} is the actuation limit at the nth actuator and T_{An}^{G} is the gravity load at the nth actuated joint. The relationship between T_{An} and $\boldsymbol{T}_u$ is obtained from Eq. (10) as

$$T_{An} = [\boldsymbol{G}_A^u]_{:n}^T \boldsymbol{T}_u \tag{A2}$$

where $[\boldsymbol{G}_A^u]_{:n}$ is the nth column vector of $[\boldsymbol{G}_A^u]$. Now, we want T_u which simultaneously satisfies the constraint Eq. (A2) and minimize $\| \boldsymbol{T}_u \|_2$, defined as

$$\| \boldsymbol{T}_u \|_2 = (\boldsymbol{T}_u^T [\boldsymbol{W}] \boldsymbol{T}_u)^{1/2} \tag{A3}$$

where $[\boldsymbol{W}]$ is a weighting matrix. Finally, maximum allowable load is obtained as below.

$$(T_u)_{\max} = (T_{An})_{\text{ext}} ([\boldsymbol{G}_A^u]_{:n}^T [\boldsymbol{W}]^{-1} [\boldsymbol{G}_A^u]_{:n})^{-1/2} \tag{A4}$$

where $(T_{An})_{\text{ext}}$ is given as

$$(T_{An})_{\text{ext}} = \min\{ |(T_{An})_{\min}|, |(T_{An})_{\max}| \} \tag{A5}$$

The above results must be evaluated for $n = 1, 2, \cdots, 6$. The smallest for the values of $(T_u)_{\max}$ is defined as the maximum load handling capacity.

Maximum Hand Velocity is defined as *the smallest maximum velocity magnitude at the end-effector such that none of actuation limits are exceeded regardless of the direction of the velocity vector, when the acceleration at the end-effector is zero* (Lee, *et. al.*, 1995).

When $\ddot{\boldsymbol{u}}$ is zero, the inertial force at the nth actuated joint is obtained from Eq. (16), as

$$T_{An} = \dot{\boldsymbol{u}}^T [\boldsymbol{P}_{Auu}^*]_{n::} \dot{\boldsymbol{u}} \tag{A6}$$

where $[\boldsymbol{P}_{Auu}^*]_{n::}$ is the nth plane of $[\boldsymbol{P}_{Auu}^*]$. The magnitude of $\dot{\boldsymbol{u}}$ is defined as

$$\dot{u} = \| \dot{\boldsymbol{u}} \|_2 = (\dot{\boldsymbol{u}}^T [\boldsymbol{W}] \dot{\boldsymbol{u}})^{1/2} \tag{A7}$$

Then, the ratio between T_{An} and $\dot{u}$ can be represented as follows.

$$(\lambda_n)_{\min} \le \frac{T_{An}}{\dot{u}^2} = \frac{\boldsymbol{e}^T [\boldsymbol{W}]^{-1} [\boldsymbol{P}_{Auu}^*]_{n::} \boldsymbol{e}}{\boldsymbol{e}^T \boldsymbol{e}} \le (\lambda_n)_{\max} \tag{A8}$$

where $\boldsymbol{e}$ is a unit vector, and $(\lambda_n)_{\min}$ and $(\lambda_n)_{\max}$ are the minimum and maximum eigenvalues of symmetric matrix of Eq. (A9), respectively.

$$\frac{1}{2}[W]^{-1}([P^*_{Auu}]_{n::}+[P^*_{Auu}]^T) \tag{A9}$$

Therefore, the maximum velocity is obtained as

$$(\dot{u})_{\max} = \left\{ \min\left(\frac{(T_{An})_{\min}}{(\lambda_n)_{\min}}, \frac{(T_{An})_{\max}}{(\lambda_n)_{\max}} \right) \right\}^{1/2} \tag{A10}$$

$(\dot{u})_{\max}$ must be evaluated for each actuated joint and the smallest value of them is defined as the maximum hand velocity.

Maximum Hand Acceleration is defined as *the smallest maximum acceleration magnitude at the end-effector such that none of actuation limits are exceeded regardless of the direction of the acceleration vector, when the velocity at the end-effector is zero* (Lee, et. al., 1995).

When $\dot{u}$ is zero, the inertial force at the nth actuated joint is obtained from Eq. (16) as

$$T_{An}=[I^*_{Au}]_{n:}\ddot{u} \tag{A11}$$

where $[I^*_{Au}]_{n::}$ is the nth row vector of $[I^*_{Au}]$. Employing the same algorithm as the load hadling capacity, the maximum acceleration at the end-effector is obtained as

$$(\ddot{u})_{\max} = (T_{An})_{\text{ext}}\{ [I^*_{Au}]_{n:}[W]^{-1}[I^*_{Au}]^T_{n:} \}^{-1/2} \tag{A12}$$

$(\ddot{u})_{\max}$ must be evaluated for each actuated joint and the smallest value of them is defined as the maximum hand acceleration.